To appear in *Advanced Robotics*
Vol. 00, No. 00, Month 20XX, 1–22

Human-Centered Control Scheme for Delayed Bilateral Teleoperation of Mobile Robots

Franco Penizzotto [a*], Emanuel Slawiñski[a] , Lucio R. Salinas[a] and Vicente A. Mut [a]

[a] *Instituto de Automática (INAUT), UNSJ-CONICET*
Avda. San Martín oeste 1109 - J5400ARL, San Juan, Argentina

(*March 2015*)

Teleoperation task performance strongly depends on how well the human operator's commands are executed. In this paper, we propose a control scheme for delayed bilateral teleoperation of mobile robots that considers user's commands execution in order to achieve a high performance teleoperation system in some important aspects like time to complete the task, safety and operator dependence. We describe some evaluation metrics that allow us to address these aspects and a quantitative metric is proposed and incorporated in the control scheme to compensate wrong commands. A force feedback is applied to the master at the local site as a haptic cue. In addition, the system stability is analyzed taking into consideration the master and remote robot dynamic models and the asymmetric time-varying delays of the communication channel. Multiple human-in-the-loop (HITL) simulations were carried out and the results of the evaluation metrics were discussed. Additionally, we present experiments where a user tele-operates a mobile robot via Internet connection between Argentina and Italy.

Keywords: Human-robot interaction, command performance, bilateral teleoperation, force feedback, time-delay, mobile robot.

1. Introduction

Robot teleoperation allows the execution of different tasks in remote environments including possibly dangerous and harmful jobs for the human operator [1]. Thus, several control schemes and strategies for mobile robot teleoperation have been developed in order to solve different tasks, e.g., land surveying in inaccessible or remote sites, transportation and storage of hazardous material, inspection of high-voltage power lines, de-activation of explosive devices, high-risk fire control, pesticide and fertilizer crop spraying and dusting, mining exploration, and others [2], [3], [4], [5] , [6], [7], [8].

The use of the Internet as a communication channel increases the application of teleoperation systems. However, it is known that the presence of time delay can induce instability or poor performance in a teleoperation system ([9], [10], [11]) as well as a poor transparency ([12]). Also the human operator's commands can be seriously affected by delayed perception of the remote environment. Moreover, commands can be very varied due to different levels of expertise, workload, distraction, attention, etc. Visual feedback can often be limited by the on-board camera restrictions, e.g., field of view, focal distance and poor resolution. Erroneous commands can induce undesired movements increasing collision probability with remote obstacles or other robots. Supplying haptic cueing in the local site (like force feedback) can mitigate some of these problems.

Generally, *good decisions* will lead to *good outcomes* and, on the contrary, *bad decisions* lead to *bad outcomes* [13]; nonetheless, sometimes an operator can correctly select the control actions but execute them poorly by over-correcting, losing control or flipping the commands.

*Corresponding author. Email: fpenizzotto@inaut.unsj.edu.ar

1.1. *Previous Work*

Recent years have seen an increase in the development of bilateral teleoperation algorithms (like [14] and [15]). Teleoperation of a robot, avoiding obstacle under time variant delays is a difficult task, even more for inexpert users or for any human operator under visual or cognitive distractions, workload or attending secondary task. Papers like [16] and [17] are focused on achieving bilateral force feedback teleoperation for a mobile robots, but they do not consider channel delays nor any human factors such as the human command performance. Some researchers have focused their attention in the human operator's commands due to the overall teleoperation task performance relies on them. [18] presented a survey covering human performance issues and suggested mitigation solutions for teleoperated systems. But still, few works have addressed the case of including in the control loop new metrics about command execution. [19] proposed a collision avoidance algorithm using an impedance force control method in which distance between a mobile robot and an obstacle is considered as a virtual force. A similar method based on this kind of impedance was used in [20], where command fusion at the remote site and a force feedback at the local site were proposed in order to help the human operator. Force reflection based on remote impedance due to fictitious force was considered in [21]. [22] achieved useful human-centered design and evaluation about haptic cueing to help the operator in a teleoperation of multiple robots. In addition, [23] presented a strategy based on a virtual reflection force that is generated to avoid obstacles and then is transferred to the joystick as a force feedback. Other approach presents a new force rendering algorithm with variable feedback gain [24], this gain depends on measured distances to the obstacles and derivatives of these distances. Although the mentioned proposals act over both the local controller (as force feedback or haptic cues) and remote controller (as force impedance), they do not change according any human performance measurement. Additionally, in [25] an approach to impedance based on a command execution metric was presented, which represents a recent approach to the inclusion of a human performance measurement, but the system does not consider time delays and only simulations were performed.

1.2. *Contribution*

The aim of this work is to *propose a control scheme for delayed bilateral teleoperation of mobile robots considering risk-based performance of the human operator's commands*. The remote impedance law and the local force feedback have influence each time a human operator's command with poor performance occurs. At the remote site, a PD-like control scheme to achieve velocity tracking and a variable impedance law to avoid obstacles (based on fictitious force) are proposed. The impedance law changes according to the user's command performance in regard to risk. At local site, a force feedback law, which also depends on the user's command performance, is considered. This is different from the current state of the art because our proposal includes on-line evaluation of commands execution in order to improve the performance of the entire system. Besides, a novel metric to quantify the user's action regarding risk is proposed. It estimates how much worse the risk level will get as a result of the current commands. Lyapunov's stability theory is first employed to prove the stability of the resulting teleoperation system, considering the dynamics of the master device and slave robot as well as time-varying delays. Then, effectiveness of the controller is validated via experimental studies, after introducing some metrics for mobile robot teleoperation tasks. Furthermore, the controller is tested through experiences over the Internet, in which a user tele-operates a mobile robot in presence of time delay, avoiding obstacles and feeling a force feedback as a haptic cue. These experiments are used to compare the performance of the proposed teleoperation system for different controllers.

This work is organized as follows: In section 2 we present the preliminaries and in section 3 we expose the control architecture. The metric to estimate the performance of the command execution is presented in section 4 and the stability analysis is shown in section 5. Then, in section 6 some performance measures are proposed in order to evaluate the system. Next, in section 7 and 8 several

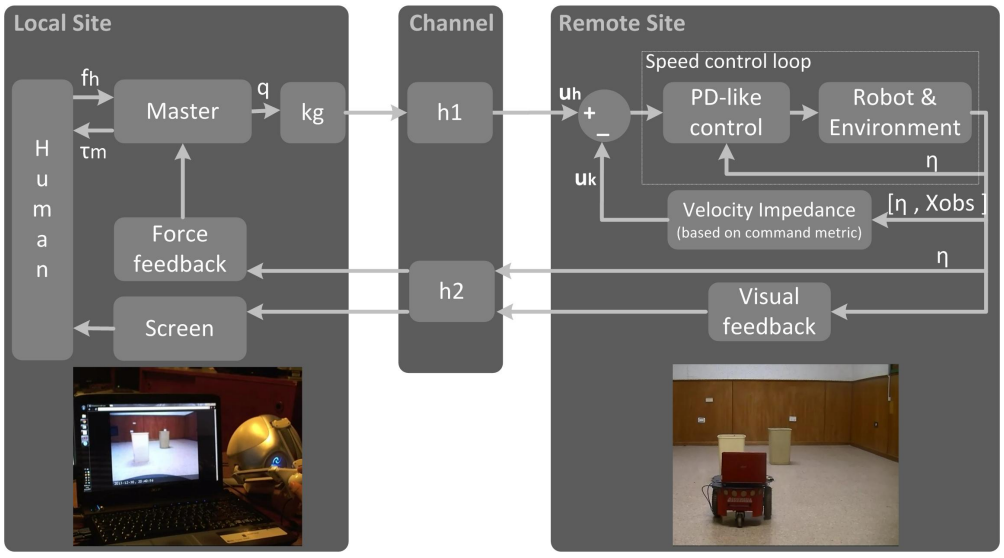

Figure 1. Bilateral teleoperation scheme. Control applied to the mobile robot and haptic feedback

experiments are shown and discussed. Finally, conclusions are exposed in section 9.

2. Preliminary

This paper proposes and analyses a teleoperation system in which a human operator drives a wheeled robot in an unknown environment using a master device (figure 1). He or she perceives the remote environment through force and visual feedback. The haptic cue in the master allows the human to feel differences in the synchronism between the local (desired speed) and remote site (robot speed). Additionally, a risk-based command performance metric is computed to change the gain of an impedance law in order to avoid obstacles.

At the local site, a three degree-of-freedom (3DOF) haptic master device is used (only 2DOF were considered, i.e., $n = 2$). The typical nonlinear dynamic model is employed, this is,

$$\mathbf{M_m}(\mathbf{q_m})\ddot{\mathbf{q}}_\mathbf{m} + \mathbf{C}(\mathbf{q_m}, \dot{\mathbf{q}}_\mathbf{m})\dot{\mathbf{q}}_\mathbf{m} + \mathbf{g}(\mathbf{q_m}) = \boldsymbol{\tau_m} + \mathbf{f_h} \tag{1}$$

where $\mathbf{q_m}(t) = [q_{m_1}(t) \;\; q_{m_2}(t)]^{\mathrm{T}}$ is the joint position of the master; $\dot{\mathbf{q}}_\mathbf{m}(t) = [\dot{q}_{m_1}(t) \;\; \dot{q}_{m_2}(t)]^{\mathrm{T}}$ is the joint velocity; $\mathbf{M_m}(\mathbf{q_m}) \in \Re^{nxn}$ is the inertia matrix; $\mathbf{C}(\mathbf{q_m}, \dot{\mathbf{q}}_\mathbf{m}) \in \Re^{nxn}$ is the matrix representing centripetal and Coriolis torques; $\mathbf{g}(\mathbf{q_m}) \in \Re^{nx1}$ is the gravitational torque; $\mathbf{f_h} \in \Re^{nx1}$ is the torque caused by the human operator force, and $\boldsymbol{\tau_m} \in \Re^{nx1}$ is the control torque applied to the master (see section 3.2).

It is common to analyze the stability of a delayed bilateral teleoperation system considering a passive model of the human operator ([26], [27]); in our case, a perturbed passive model is used which is described by:

$$\mathbf{f_h} = -k_h\mathbf{q_m} - \alpha_h\dot{\mathbf{q}}_\mathbf{m} + \mathbf{f_a} \tag{2}$$

where k_h and α_h are positive intrinsic parameters of the human operator, and $\mathbf{f_a}$ is the active component of $\mathbf{f_h}$.

At the remote site, the dynamic model of a unicycle-type mobile robot is considered as the slave. It has two independently actuated rear wheels and is represented by,

$$\mathbf{D}\dot{\boldsymbol{\eta}} + \mathbf{Q}(\boldsymbol{\eta})\boldsymbol{\eta} = \boldsymbol{\tau_s} + \mathbf{f_e} \tag{3}$$

where $\boldsymbol{\eta} = [\eta_1 \quad \eta_2]^{\mathrm{T}}$ is the robot velocity vector with η_1 and η_2 representing the linear and angular velocity of the mobile robot respectively, $D = \left[\begin{smallmatrix} m & 0 \\ 0 & i_n \end{smallmatrix}\right]$ is the inertia matrix, $Q = \left[\begin{smallmatrix} 0 & -ma\eta_2 \\ ma\eta_2 & 0 \end{smallmatrix}\right]$ is the Coriolis matrix, m is the mass of the robot, i_n is the rotational inertia, and a is the distance between the mass center and the geometric center. In addition, $\boldsymbol{\tau_s} = [u_1 \quad u_2]$ involves a control force u_1 and a control torque u_2 (see section 3.1). $\mathbf{f_e}$ is the force and torque caused by the elements of the environment on the robot. In our case, since the robot should avoid obstacles, $\mathbf{f_e}$ is formed by fictitious force and torque components (tangential and normal),

$$\mathbf{f_e} = [f_t \quad f_y]^{\mathrm{T}} \tag{4}$$

that depend on the robot-obstacle distance (shown afterwards in section 3.1.1).

Furthermore, the communication channel adds a forward time delay h_1 (from the master to the slave) and a backward time delay h_2 (from the slave to the master). Generally, these delays are time-varying and forward and backward delays differ (asymmetric delays).

2.1. *Properties, assumptions and lemma*

The following ordinary properties, assumptions and lemma will be used in this paper:

Property 1: The inertia matrices $\mathbf{M_m}(\mathbf{q_m})$ and $\mathbf{D}$ are symmetric positive definite.

Property 2: The matrix $\dot{\mathbf{M}}_{\mathbf{m}}(\mathbf{q_m}) - 2\mathbf{C_m}(\mathbf{q_m}, \dot{\mathbf{q}}_{\mathbf{m}})$ is skew-symmetric.

Property 3: There exists a $k_c > 0$ such that $\mathbf{C_m}(\mathbf{q_m}, \dot{\mathbf{q}}_{\mathbf{m}})\dot{\mathbf{q}}_{\mathbf{m}} \leq k_c|\dot{\mathbf{q}}_{\mathbf{m}}|$.

Assumption 1: The time delays $h_1(t)$ and $h_2(t)$ are bounded. Therefore, there exist positive scalars $\bar{h}_1$ and $\bar{h}_2$ such that $0 \leq h_1(t) \leq \bar{h}_1$ and $0 \leq h_2(t) \leq \bar{h}_2$ for all t.

Assumption 2: The environment force/torque and the non-passive component of the human force are bounded, this is $|\mathbf{f_e}| \leq \bar{f}_e$ and $|\mathbf{f_a}| \leq \bar{f}_a$ where $\bar{f}_e$ and $\bar{f}_a$ are positive values.

Lemma 1 ([27])**:** For real vector functions $\mathbf{a}(.)$ and $\mathbf{b}(.)$ and a time-varying scalar $h(t)$ with $0 \leq h(t) \leq \bar{h}$, the following inequality holds,

$$-2\mathbf{a}^{\mathrm{T}}(t)\int_{t-h(t)}^{t}\mathbf{b}(\xi)d\xi - \int_{t-h(t)}^{t}\mathbf{b}^{\mathrm{T}}(\xi)\mathbf{X}\mathbf{b}(\xi)\,d\xi \;\leq\; h(t)\,\mathbf{a}^{\mathrm{T}}(t)\,\mathbf{X}^{-1}\mathbf{a}(t) \leq \bar{h}\mathbf{a}^{\mathrm{T}}(t)\,\mathbf{X}^{-1}\mathbf{a}(t) \tag{5}$$

where $\mathbf{X} > 0$ is a positive definite matrix.

3. Control Scheme

Recent researches like [26], [27] and [28] present control schemes for teleoperation of manipulator robots based on PD-like structures. They have proved asymptotic stability of these schemes by using a sufficiently large damping injected into the master and slave. We propose to extend a similar structure to mobile robot teleoperation.

3.1. *Remote Site*

The control action applied to the mobile robot at the remote site is established as follows:

$$\boldsymbol{\tau_s} = k_s((k_g\mathbf{q_m}(t-h_1) - \mathbf{u_k}) - \boldsymbol{\eta}) - \alpha_s\mathbf{z} + \mathbf{Q}(\boldsymbol{\eta})\boldsymbol{\eta} \tag{6}$$

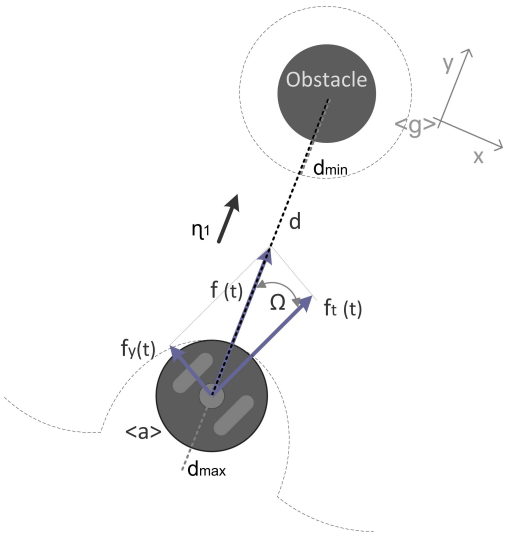

Figure 2. Fictitious force vector

where

$$\mathbf{u_k} = sgn(\mathbf{q_m}(t-h1))u_m(1-e^{-(\varepsilon+C_{Met})k_f\mathbf{f_e}}) \tag{7}$$

being $\boldsymbol{\tau_s}$ the force/torque applied to the robot. $\mathbf{u_k} \in \Re^{nx1}$ is the velocity impedance (see section 3.1.1), k_g is a gain that maps master position to velocity command, k_s and α_s are positive constants and they represent the proportional gain and acceleration dependent damping of the velocity controller respectively. In addition, C_{Met} is a risk-based metric or performance index (see section 4), and ε, u_m and k_f are positive constants tuned by the designer (after being adjusted and considering the maximum $\mathbf{f_e}$, $\mathbf{u_k}$ should go from a minimum to u_m while C_{Met} goes from 0 to 1).

Furthermore, $\mathbf{z}$ is defined by,

$$\dot{\boldsymbol{\eta}} = \mathbf{z} + \gamma\dot{\mathbf{z}} \tag{8}$$

with $\gamma \to 0^+$. The signal $\mathbf{z}$ represents the mobile robot acceleration $\dot{\boldsymbol{\eta}}$ at an infinitesimal time instant before t so it is assumed $\dot{\boldsymbol{\eta}} \approx \mathbf{z}$ considering $\dot{\mathbf{z}}$ without discontinuities.

3.1.1. Velocity Impedance

As it was previously mentioned, a velocity impedance law was used in many control schemes to avoid obstacles, but in this work we propose to use a risk-based variable impedance that depends on a performance index proposed in this work. In [25] we have discussed and proved the advantages of using a variable gain in the impedance law in a mobile robot teleoperation system.

Figure 2 shows a graphical representation of the fictitious force/torque vector, generated from the robot-obstacle interaction. $d(t)$ is the distance between the robot and the obstacle and the fictitious force/torque vector $\mathbf{f_e} = [f_t \quad f_y]^{\mathrm{T}}$ is decomposed in two components that affect the linear and angular speed impedance signals. $f(t) = a - b\ d(t)$, with a and b as positive constant such that $a - bd_{max} = 0$ and $a - bd_{min} = 1$. d_{min} and d_{max} are the minimum and maximum distances that confine the impedance zone, adjusted by the designer. Then, $f_t(t) = f(t)\cos\Omega(t)$ and $f_y(t) = f(t)\sin\Omega(t)$, where $\Omega(t)$ is the angle between $f(t)$ and $f_t(t)$. A similar equation for the fictitious force/torque vector is described in [29].Finally, $< a >$ is the reference frame of the robot velocities while $< g >$ is the reference frame of the fictitious forces.

3.2. *Local Site*

In the literature, three classes of haptic cues are typically considered as force feedback sources in conventional teleoperation systems: 1) The mismatch between the command of the master and the execution of the slave in terms of position or velocity, which is called master-slave tracking error; 2) the force measured by a force sensor mounted on the slave in contact with the environment; 3) a linear combination of both [30]. Generally, a PD control control law is applied to the first error mentioned while a P control is suitable for the second error.

In our case, some considerations should be taken into account. First, the master-slave tracking error, as defined above, cannot be directly applied given that the desired robot speed is proportional to $\mathbf{q_m}$ rather than $\dot{\mathbf{q}}_\mathbf{m}$ in accordance with our control scheme. Second, there is no real contact force acting on the slave side, so, there is not a real $\mathbf{f_e}$. The velocity impedance $\mathbf{u_k}$ increases the master-slave tracking error, hence, the command metric is indirectly feedbacked to the human operator. Therefore, we define our force feedback control as,

$$\boldsymbol{\tau_m} = -k_m(k_g\mathbf{q_m} - \boldsymbol{\eta}(t-h_2)) - \alpha_m\dot{\mathbf{q}}_\mathbf{m} + \mathbf{g}(\mathbf{q_m}) \tag{9}$$

where $\boldsymbol{\tau_m}$ is the torque applied to the master, α_m is the damping injected into the master, k_m is the gain of the force applied to the master to reduce the synchronization error. The first term of this haptic cue corresponds to the mismatch between the commanded velocity (specified by $k_g\mathbf{q_m}$) and the real robot velocity, which can occur for multiple reasons: 1) Robot-related: imprecise parameter calibration of robot's speed controller, big inertias, etc.; 2) External disturbances; and 3) Velocity impedance.

4. Measure of human performance

4.1. *Risk-based metric definition*

In this section, we propose a metric or performance index C_{Met} to quantify some aspects of the human operator's commands during the teleoperation task. We define C_{Met} as *"the degree of potential worsening of the robot-obstacle collision risk at the remote site, caused by the delayed commands of the human operator"*.

In order to achieve a quantitative method for the risk-based metric, the following terms are established:

- Real risk ($Pr(t)$):
  Level of risk produced as an effect of the robot-obstacle interaction.
- Command risk ($Pc(t)$):
  Level of risk produced as an effect of the robot-obstacle interaction that *would* appear after the application of the operator's commands during an interval of time (integration time, T_{int}).

Figure 3 shows a situation where the time delay is not taken into account in order to simplify the explanation of the proposal. The real robot (Real Robot, RR) appears in solid dark gray at t_n, and its past position is shown in solid light gray (at t_{n-1} and t_{n-2}). In addition, progression of the real robot based on the current velocity components ($\dot{x}_r$ and $\dot{y}_r$) is illustrated in black dotted lines (Virtual Real Robot, VRR). The progression is considered for an integration time T_{int}, with Δ_t as step time and j is a subindex ($0 \leq j \in \aleph \leq \frac{T_{int}}{\Delta_t}$). The same situation is represented for an obstacle (square, Virtual Obstacle, VO). Of course, in order to achieve a better estimation of the trajectories, an algorithm based on actual and past velocities can be used.

Furthermore, the robots in solid line correspond to the estimated progression for the real robot considering new commands applied at t_n (Virtual Command Robot, VCR). An approximated model of the robot is considered to simplify the computation.

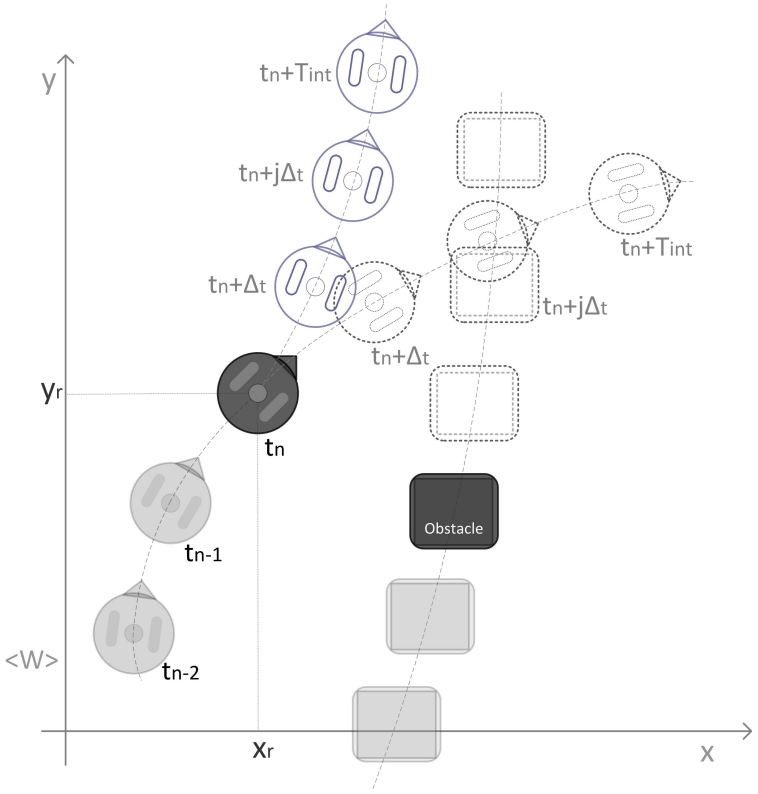

Figure 3. Components of the proposed method

In order to enhance the understanding of the method, let us consider the robot system at a stationary point before $t = t_n$, and at $t = t_n$ the user change the velocity command. At t_n, velocity components of the robot are $((\dot{x}_r(t_n)\ , \dot{y}_r(t_n))$, which are used to estimate a virtual trajectory for the next interval of integration (the command at t_n do not take participation in these trajectories). On the other hand, the computation of the trajectory for the VCR (virtual command robot) is made after estimating $\dot{x}_c$ and $\dot{y}_c$ (velocity components of VCR), using a dynamic model of the robot. $\dot{x}_{obs}$ and $\dot{y}_{obs}$ represent the components of the velocity of the obstacle.

Then, for each j, contact times between VRR-VO and VCR-VO are estimated. The minimum time of each one correspond to the contact times of the interactions VRR-VO and VCR-VO at the actual time t_n, respectively.

4.2. *Method to Signal*

At t_n, for each step j of the integration time T_{int}, the next equations are computed, using the robot and obstacle positions and velocities at t_n :

Virtual trajectory for the VRR:

$$\begin{cases} x_r(t_n + (j+1)\Delta_t) = \dot{x}_r(t_n)\Delta_t + x_r(t_n + j\Delta_t) \\ y_r(t_n + (j+1)\Delta_t) = \dot{y}_r(t_n)\Delta_t + y_r(t_n + j\Delta_t) \end{cases} \tag{10}$$

Virtual trajectory for the VO:

$$\begin{cases} x_{obs}(t_n + (j+1)\Delta_t) = \dot{x}_{obs}(t_n)\Delta_t + x_{obs}(t_n + j\Delta_t) \\ y_{obs}(t_n + (j+1)\Delta_t) = \dot{y}_{obs}(t_n)\Delta_t + y_{obs}(t_n + j\Delta_t) \end{cases} \tag{11}$$

In addition, virtual trajectory for the VCR:

$$\begin{cases} x_c(t_n + (j+1)\Delta_t) = \dot{x}_c(t_n + j\Delta_t)\Delta_t + x_c(t_n + j\Delta_t) \\ y_c(t_n + (j+1)\Delta_t) = \dot{y}_c(t_n + j\Delta_t)\Delta_t + y_c(t_n + j\Delta_t) \end{cases} \tag{12}$$

being the dynamic model:

$$\begin{cases} u(t_n + j\Delta_t) = u_{ref}(t_n)e^{-a(t_n+j\Delta_t)} \\ \omega(t_n + j\Delta_t) = \omega_{ref}(t_n)e^{-a(t_n+j\Delta_t)} \\ \dot{x}_c(t_n + j\Delta_t) = u(t_n + j\Delta_t)\cos(\phi(t_n + j\Delta_t)) + x_c(t_n + j\Delta_t) \\ \dot{y}_c(t_n + j\Delta_t) = u(t_n + j\Delta_t)\sin(\phi(t_n + j\Delta_t)) + y_c(t_n + j\Delta_t) \\ \dot{\phi}(t_n + j\Delta_t) = \omega(t_n + j\Delta_t) \end{cases} \tag{13}$$

with $a > 0$ (its value depends on the dynamics of the robot's closed-loop speed control), $u_{ref}(t_n) = k_g q_{m_1}(t_n - h_1)$ and $\omega_{ref}(t_n) = k_g q_{m_2}(t_n - h_1)$. Additionally, u, w and ϕ are the linear velocity, angular velocity and orientation angle of the robot respectively; q_{m_1} and q_{m_2} are the joints position of the master (see eq. (1).)

Next, some variables are defined:

Real risk, $P_r(t_n)$: Distance between the VRR and VO (Dst_{ro}), for each step time during the integration time, is computed as,

$$Dst_{ro}(t_n + j\Delta_t) = \|(x_r(t_n + j\Delta_t), y_r(t_n + j\Delta_t)) - (x_{obs}(t_n + j\Delta_t), y_{obs}(t_n + j\Delta_t))\| \tag{14}$$

then, the following conditional is applied:

$$if(Dst_{ro}(t_n + j\Delta_t) < Dst_{min}) \Rightarrow \begin{cases} P_r(t_n) = 1 - \frac{j\Delta_t}{T_{int}} \\ StpInt_r = 1 \end{cases} \tag{15}$$

where $Dst_{min} = Rad_r + Rad_{obs} + \varepsilon_{dst}$ is a robot-obstacle contact distance, Rad_r and Rad_{obs} the radius of the robot and obstacle respectively, and $\varepsilon_{dst} > 0$ a tuning parameter. $StpInt_r$ is a binary variable used to indicate to stop the $P_r(t_n)$ algorithm. Estimating the collision probability (P_r) as a function of time-to-contact was previously introduced in [31].

Command risk, $P_c(t_n)$: Distance between the VCR and VO (Dst_{co}), for each step time during the integration time, is computed as,

$$Dst_{co}(t_n + j\Delta_t) = \|(x_c(t_n + j\Delta_t), y_c(t_n + j\Delta_t)) - (x_{obs}(t_n + j\Delta_t), y_{obs}(t_n + j\Delta_t))\| \tag{16}$$

then, the following conditional is applied:

$$if(Dst_{co}(t_n + j\Delta_t) < Dst_{min}) \Rightarrow \begin{cases} P_c(t_n) = 1 - \frac{j\Delta_t}{T_{int}} \\ StpInt_c = 1; \end{cases} \tag{17}$$

where the binary variable $StpInt_c$ indicates to stop the $P_c(t_n)$ algorithm.

Considering this metric proposal is about risk, we are interested in high values of the collision probabilities rather than lower ones. So, a cost function (J) based on the square of the collision probability is chosen because it enhances high values of risk.

Taking (15) and (17) the next cost functions are defined:

Cost function for VRR,

$$J_r(t_n) = P_r^2(t_n) \tag{18}$$

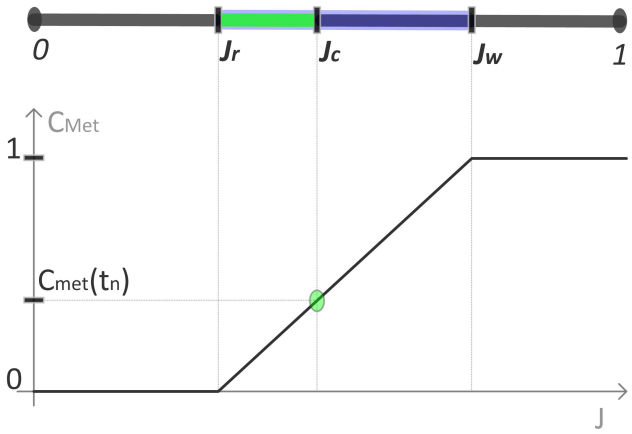

Figure 4. Evaluation of the proposed metric C_{Met}

Cost function for VCR,

$$J_c(t_n) = P_c^2(t_n) \tag{19}$$

Worst cost function,

$$J_w(t_n) = 1 \tag{20}$$

The cost function J_w is considered constant for simplicity, taking into account that the worst situation is the one with high collision probability. In a future work, J_w can be computed with an optimization algorithm, which should compute the worst collision probability for possible commands.

For each t_n, it can be deduced that when $J_c < J_r$, the command will improve the actual cost function, therefore $C_{Met} = 0$. On the other hand, when $J_c > J_r$, the situation considering risk is going to get worse in the near future. Eq. (21) shows the mathematical form:

$$\begin{cases} C_{Met_{obs}} = 0 \ , & if \quad J_c < J_r \\ C_{Met_{obs}} = \frac{J_c - J_r}{J_w - J_r} \ , & if \quad J_r < J_c < J_w \end{cases} \tag{21}$$

Then, for k obstacles interacting in the environment, we have

$$C_{Met} = \max\{C_{Met_{obs_1}} \ \dots \ C_{Met_{obs_k}}\} \tag{22}$$

Remark 1: in this work, the radius and position of the obstacles are considered known, but they can be estimated with a laser scanner. For the case of other mobile robots interacting in the environment, their positions can be received by a network communication.

Remark 2: Eq. (22) could be replaced for a more complex one, which should combine all the C_{Met} elements in a reasonable way.

5. System Stability analysis

It is important to highlight the common states variables that should be analyzed in a teleoperation system. They are: the master-slave tracking error, the master velocity and the slave velocity (indirectly through the master position and tracking error in this work). Because our remote controller implementation, the filtered acceleration of the slave ($\mathbf{z}$) is also analyzed.

Initially, a positive definite functional $V_i = V_1 + V_2 + V_3 + V_4 + V_5 > 0$ is proposed. It is important to remark that there is not an equilibrium point but a Krasovskii-like equilibrium solution that depends on the state $\mathbf{x}^{\mathrm{T}} = [\dot{\mathbf{q}}_{\mathbf{m}}^{\mathrm{T}} \ \ (\boldsymbol{\eta} - k_g \mathbf{q}_{\mathbf{m}})^{\mathrm{T}} \ \ \mathbf{z}^{\mathrm{T}} \ \ \mathbf{q}_{\mathbf{m}}^{\mathrm{T}}]$ in the time interval $[t - h_1 - h_2, t]$ [32, 33].

Remark 3: The common (t) is no explicit for variables depending of the current time, but it is explicit for delayed variables.

The functional is formed by five parts: V_1 and V_3 represent the motion energy of the master and mobile robot, V_2 represents the potential energy of the error between the master and the mobile robot, V_4 represents the potential energy of the master, and V_{5_i} is included for mathematical reasons in order to transform the terms that include delayed variables to terms with non-delayed variables. The first four sub-functional are proposed in the following manner:

$$V_1 = \frac{1}{2}\frac{k_g}{k_m}\dot{\mathbf{q}}_{\mathbf{m}}^{\mathrm{T}}\mathbf{M}_{\mathbf{m}}\left(\mathbf{q}_{\mathbf{m}}\right)\dot{\mathbf{q}}_{\mathbf{m}} \tag{23}$$

$$V_2 = \frac{1}{2}\left(\boldsymbol{\eta} - k_g\mathbf{q}_{\mathbf{m}}\right)^{\mathrm{T}}\left(\boldsymbol{\eta} - k_g\mathbf{q}_{\mathbf{m}}\right) \tag{24}$$

$$V_3 = \frac{1}{2}\gamma\mathbf{z}^{\mathrm{T}}\mathbf{z} \tag{25}$$

$$V_4 = \frac{1}{2}\frac{k_h k_g}{k_m}\mathbf{q}_{\mathbf{m}}^{\mathrm{T}}\mathbf{q}_{\mathbf{m}} \tag{26}$$

The time derivative of V_1 along the master dynamics (1), taking into account properties 1 and 2, is the following one,

$$\begin{aligned}
\dot{V}_1 &= \frac{1}{2}\frac{k_g}{k_m}\dot{\mathbf{q}}_{\mathbf{m}}^{\mathrm{T}}\dot{\mathbf{M}}_{\mathbf{m}}\dot{\mathbf{q}}_{\mathbf{m}} + \frac{k_g}{k_m}\dot{\mathbf{q}}_{\mathbf{m}}^{\mathrm{T}}\mathbf{M}_{\mathbf{m}}\ddot{\mathbf{q}}_{\mathbf{m}} \\
&= \frac{1}{2}\frac{k_g}{k_m}\dot{\mathbf{q}}_{\mathbf{m}}^{\mathrm{T}}\dot{\mathbf{M}}_{\mathbf{m}}\dot{\mathbf{q}}_{\mathbf{m}} + \ \frac{k_g}{k_m}\dot{\mathbf{q}}_{\mathbf{m}}^{\mathrm{T}}\mathbf{M}_{\mathbf{m}}\mathbf{M}_{\mathbf{m}}^{-1}\left(\boldsymbol{\tau}_{\mathbf{m}} + \mathbf{f}_{\mathbf{h}} - \mathbf{C}_{\mathbf{m}}\dot{\mathbf{q}}_{\mathbf{m}} - \mathbf{g}_{\mathbf{m}}\right) \\
&= \frac{k_g}{k_m}\dot{\mathbf{q}}_{\mathbf{m}}^{\mathrm{T}}\left(\boldsymbol{\tau}_{\mathbf{m}} + \mathbf{f}_{\mathbf{h}} - \mathbf{g}_{\mathbf{m}}\right)
\end{aligned} \tag{27}$$

Now, if the control action $\boldsymbol{\tau}_{\mathbf{m}}$ (9) is included in (27), and considering (2), it yields,

$$\begin{aligned}
\dot{V}_1 &= \frac{k_g}{k_m}\dot{\mathbf{q}}_{\mathbf{m}}^{\mathrm{T}}\left(\boldsymbol{\tau}_{\mathbf{m}} - \mathbf{g}_{\mathbf{m}}\right) + \frac{k_g}{k_m}\dot{\mathbf{q}}_{\mathbf{m}}^{\mathrm{T}}\mathbf{f}_{\mathbf{h}} \\
&= \frac{k_g}{k_m}\dot{\mathbf{q}}_{\mathbf{m}}^{\mathrm{T}}(-k_m\left(k_g\mathbf{q}_{\mathbf{m}} - \boldsymbol{\eta}\left(t - h_2\right)\right) - \ \left(\alpha_m + \alpha_h\right)\dot{\mathbf{q}}_{\mathbf{m}}) + \frac{k_g}{k_m}\dot{\mathbf{q}}_{\mathbf{m}}^{\mathrm{T}}\mathbf{f}_{\mathbf{a}} - \frac{k_h k_g}{k_m}\dot{\mathbf{q}}_{\mathbf{m}}^{\mathrm{T}}\mathbf{q}_{\mathbf{m}} \\
&= -k_g\dot{\mathbf{q}}_{\mathbf{m}}^{\mathrm{T}}(k_g\mathbf{q}_{\mathbf{m}} - \boldsymbol{\eta}\left(t - h_2\right) + \boldsymbol{\eta} - \boldsymbol{\eta}) - \ \left(\alpha_m + \alpha_h\right)\frac{k_g}{k_m}\dot{\mathbf{q}}_{\mathbf{m}}^{\mathrm{T}}\dot{\mathbf{q}}_{\mathbf{m}} + \frac{k_g}{k_m}\dot{\mathbf{q}}_{\mathbf{m}}^{\mathrm{T}}\mathbf{f}_{\mathbf{a}} - \ \frac{k_h k_g}{k_m}\dot{\mathbf{q}}_{\mathbf{m}}^{\mathrm{T}}\mathbf{q}_{\mathbf{m}} \\
&= k_g\dot{\mathbf{q}}_{\mathbf{m}}^{\mathrm{T}}\left(\boldsymbol{\eta} - k_g\mathbf{q}_{\mathbf{m}}\right) - k_g\dot{\mathbf{q}}_{\mathbf{m}}^{\mathrm{T}}\int_{t-h_2}^{t}\dot{\boldsymbol{\eta}}\left(\xi\right)d\xi - \ \left(\alpha_m + \alpha_h\right)\frac{k_g}{k_m}\dot{\mathbf{q}}_{\mathbf{m}}^{\mathrm{T}}\dot{\mathbf{q}}_{\mathbf{m}} + \frac{k_g}{k_m}\dot{\mathbf{q}}_{\mathbf{m}}^{\mathrm{T}}\mathbf{f}_{\mathbf{a}} - \ \frac{k_h k_g}{k_m}\dot{\mathbf{q}}_{\mathbf{m}}^{\mathrm{T}}\mathbf{q}_{\mathbf{m}}
\end{aligned} \tag{28}$$

Next, $\dot{V}_2$ along the dynamics of the wheeled robot (3) is obtained as,

$$\begin{aligned}
\dot{V}_2 &= \left(\boldsymbol{\eta} - k_g\mathbf{q}_{\mathbf{m}}\right)^{\mathrm{T}}\left(\dot{\boldsymbol{\eta}} - k_g\dot{\mathbf{q}}_{\mathbf{m}}\right) = \left(\boldsymbol{\eta} - k_g\mathbf{q}_{\mathbf{m}}\right)^{\mathrm{T}}\dot{\boldsymbol{\eta}} - k_g\left(\boldsymbol{\eta} - k_g\mathbf{q}_{\mathbf{m}}\right)^{\mathrm{T}}\dot{\mathbf{q}}_{\mathbf{m}} \\
&= k_s\left(\boldsymbol{\eta} - k_g\mathbf{q}_{\mathbf{m}}\right)^{\mathrm{T}}\mathbf{D}^{-1}(k_g\mathbf{q}_{\mathbf{m}}\left(t - h_1\right) - \mathbf{u}_{\mathbf{k}} - \boldsymbol{\eta} + \ k_g\mathbf{q}_{\mathbf{m}} - k_g\mathbf{q}_{\mathbf{m}}) - k_g\left(\boldsymbol{\eta} - \mathbf{q}_{\mathbf{m}}k_g\right)^{\mathrm{T}}\dot{\mathbf{q}}_{\mathbf{m}} \\
&\quad + \ \left(\boldsymbol{\eta} - k_g\mathbf{q}_{\mathbf{m}}\right)^{\mathrm{T}}\mathbf{D}^{-1}\mathbf{f}_{\mathbf{e}} - \ \alpha_s\left(\boldsymbol{\eta} - k_g\mathbf{q}_{\mathbf{m}}\right)^{\mathrm{T}}\mathbf{D}^{-1}\mathbf{z}
\end{aligned}$$

$$= -k_s \left(\boldsymbol{\eta} - k_g \mathbf{q_m}\right)^{\mathrm{T}} \mathbf{D}^{-1} \left(\boldsymbol{\eta} - k_g \mathbf{q_m}\right) - \ k_g \left(\boldsymbol{\eta} - k_g \mathbf{q_m}\right)^{\mathrm{T}} \dot{\mathbf{q}}_\mathbf{m} + \left(\boldsymbol{\eta} - k_g \mathbf{q_m}\right)^{\mathrm{T}} \mathbf{D}^{-1} \mathbf{f_e}$$
$$- k_s k_g \left(\boldsymbol{\eta} - k_g \mathbf{q_m}\right)^{\mathrm{T}} \mathbf{D}^{-1} \int_{t-h_1}^{t} \dot{\mathbf{q}}_\mathbf{m}(\xi) d\xi - \ \alpha_s \left(\boldsymbol{\eta} - k_g \mathbf{q_m}\right)^{\mathrm{T}} \mathbf{D}^{-1} \mathbf{z} - k_s \left(\boldsymbol{\eta} - k_g \mathbf{q_m}\right)^{\mathrm{T}} \mathbf{D}^{-1} \mathbf{u_k} \tag{29}$$

Additionally, $\dot{V}_3$ can be written including (8) and considering (3) and (6), in the following way,

$$\begin{aligned}
\dot{V}_3 &= \gamma \mathbf{z}^{\mathrm{T}} \dot{\mathbf{z}} = \gamma \mathbf{z}^{\mathrm{T}} \left(\frac{\dot{\boldsymbol{\eta}}}{\gamma} - \frac{\mathbf{z}}{\gamma} \right) = \mathbf{z}^{\mathrm{T}} \dot{\boldsymbol{\eta}} - \mathbf{z}^{\mathrm{T}} \mathbf{z} \\
&= -\alpha_s \mathbf{z}^{\mathrm{T}} \mathbf{D}^{-1} \mathbf{z} + k_s \mathbf{z}^{\mathrm{T}} \mathbf{D}^{-1} \left(k_g \mathbf{q_m}(t - h_1) - \mathbf{u_k} - \boldsymbol{\eta} \right) + \ \mathbf{z}^{\mathrm{T}} \mathbf{D}^{-1} \mathbf{f_e} - \mathbf{z}^{\mathrm{T}} \mathbf{z} \\
&= -\alpha_s \mathbf{z}^{\mathrm{T}} \mathbf{D}^{-1} \mathbf{z} - k_s \mathbf{z}^{\mathrm{T}} \mathbf{D}^{-1} \left(\boldsymbol{\eta} - k_g \mathbf{q_m} \right) - \ k_s k_g \mathbf{z}^{\mathrm{T}} \mathbf{D}^{-1} \int_{t-h_1}^{t} \dot{\mathbf{q}}_\mathbf{m}(\xi) \, d\xi + \ \mathbf{z}^{\mathrm{T}} \mathbf{D}^{-1} \mathbf{f_e} \\
&\quad - \mathbf{z}^{\mathrm{T}} \mathbf{z} - k_s \mathbf{z}^{\mathrm{T}} \mathbf{D}^{-1} \mathbf{u_k}
\end{aligned} \tag{30}$$

Below, the time derivative of V_4 is calculated,

$$\dot{V}_4 = \frac{k_h k_g}{k_m} \mathbf{q_m}^{\mathrm{T}} \dot{\mathbf{q}}_\mathbf{m} \tag{31}$$

It is possible to appreciate in (28)-(30) that there are delayed variables that make the stability analysis difficult, e.g., the term $-k_s k_g \mathbf{z}^{\mathrm{T}} \mathbf{D}^{-1} \int_{t-h_1}^{t} \dot{\mathbf{q}}_\mathbf{m}(\xi) \, d\xi$ in (30). To solve this, V_5 is proposed as follows:

$$V_5 = \int_{-\bar{h}_2}^{0} \int_{t+\theta}^{t} \mathbf{z}^{\mathrm{T}}(\xi) \mathbf{W} \mathbf{z}(\xi) \, d\xi d\theta + \int_{-\bar{h}_1}^{0} \int_{t+\theta}^{t} \dot{\mathbf{q}}_\mathbf{m}^{\mathrm{T}}(\xi) \left(\mathbf{X} + \mathbf{Y} \right) \dot{\mathbf{q}}_\mathbf{m}(\xi) \, d\xi d\theta \tag{32}$$

where $\mathbf{W}, \mathbf{X}, \mathbf{Y}$ are positive definite matrices.
From (32), and considering assumption 1, $\dot{V}_5$ can be computed by,

$$\dot{V}_5 \ \leq \ \bar{h}_2 \mathbf{z}^{\mathrm{T}} \mathbf{W} \mathbf{z} - \int_{t-h_2}^{t} \mathbf{z}^{\mathrm{T}}(\xi) \mathbf{W} \mathbf{z}(\xi) \, d\xi + \ \bar{h}_1 \dot{\mathbf{q}}_\mathbf{m}^{\mathrm{T}} \left(\mathbf{X} + \mathbf{Y} \right) \dot{\mathbf{q}}_\mathbf{m} - \int_{t-h_1}^{t} \dot{\mathbf{q}}_\mathbf{m}^{\mathrm{T}}(\xi) \left(\mathbf{X} + \mathbf{Y} \right) \dot{\mathbf{q}}_\mathbf{m}(\xi) \, d\xi \tag{33}$$

On the other hand, each term of $\dot{V}_1 + \dot{V}_2 + \dot{V}_3$ that includes a delayed variable can be conveniently joined using Lemma 1 (5) with one term of $\dot{V}_5$. Next, Eq. (34)-(36) will use this property.

Applying distributive property in the last term of (33) and then, joining the first subterm of this result with the fourth term of (29),

$$\begin{aligned}
&- \int_{t-h_1}^{t} \dot{\mathbf{q}}_\mathbf{m}^{\mathrm{T}}(\xi) \mathbf{X} \dot{\mathbf{q}}_\mathbf{m}(\xi) \, d\xi - \ k_s k_g \left(\boldsymbol{\eta} - \mathbf{q_m} \right)^{\mathrm{T}} \mathbf{D}^{-1} \int_{t-h_1}^{t} \dot{\mathbf{q}}_\mathbf{m}(\xi) \, d\xi \\
&\qquad \leq \ \tfrac{1}{4} \bar{h}_1 k_g^2 k_s^2 \left(\boldsymbol{\eta} - \mathbf{q_m} \right)^{\mathrm{T}} \mathbf{D}^{-1} \mathbf{X}^{-1} \mathbf{D}^{-1} \left(\boldsymbol{\eta} - \mathbf{q_m} \right)
\end{aligned} \tag{34}$$

Again, we apply distributive property in the last term of (33) and then, the second subterm of

this result is joined with the third term of (30),

$$-\int_{t-h_1}^{t}\dot{\mathbf{q}}_{\mathbf{m}}^{\mathrm{T}}(\xi)\,\mathbf{Y}\dot{\mathbf{q}}_{\mathbf{m}}(\xi)\,d\xi-\;k_sk_g\mathbf{z}^{\mathrm{T}}\mathbf{D}^{-1}\int_{t-h_1}^{t}\dot{\mathbf{q}}_{\mathbf{m}}(\xi)\,d\xi\;\leq\;\tfrac{1}{4}\bar{h}_1k_g^2k_s^2\mathbf{z}^{\mathrm{T}}\mathbf{D}^{-1}\mathbf{Y}^{-\mathbf{1}}\mathbf{D}^{-1}\mathbf{z}\qquad(35)$$

Now, linking the second term of (33) with the second term of (28),

$$\begin{aligned}&-\int_{t-h_2}^{t}\mathbf{z}^{\mathrm{T}}(\xi)\,\mathbf{W}\mathbf{z}(\xi)\,d\xi-k_g\dot{\mathbf{q}}_{\mathbf{m}}^{\mathrm{T}}\int_{t-h_2}^{t}\dot{\boldsymbol{\eta}}(\xi)\,d\xi\\&=-\int_{t-h_2}^{t}\mathbf{z}^{\mathrm{T}}(\xi)\,\mathbf{W}\mathbf{z}(\xi)\,d\xi-k_g\dot{\mathbf{q}}_{\mathbf{m}}^{\mathrm{T}}\int_{t-h_2}^{t}(\mathbf{z}(\xi)+\gamma\dot{\mathbf{z}}(\xi))\,d\xi\\&\leq\;\frac{1}{4}\bar{h}_2k_g^2\dot{\mathbf{q}}_{\mathbf{m}}^{\mathrm{T}}\mathbf{W}^{-1}\dot{\mathbf{q}}_{\mathbf{m}}+\gamma k_gh_2\sigma\left|\dot{\mathbf{q}}_{\mathbf{m}}\right|\end{aligned}\qquad(36)$$

In (36), the integral function is applied in a closed interval to $\dot{\mathbf{z}}(t)$ (assumed without discontinuities) therefore the function $\int_{t-h_2}^{t}\dot{\mathbf{z}}(\xi)d\xi$ has a maximum real value σ that bounds such function and then $\left|\int_{t-h_2}^{t}\dot{\mathbf{z}}(\xi)d\xi\right|\leq h_2\sigma$.

Next, joining the penultimate term of (29) and the second term of (30), the following inequality can be deduced,

$$-(\alpha_s+k_s)(\boldsymbol{\eta}-k_g\mathbf{q}_{\mathbf{m}})^{\mathrm{T}}\mathbf{D}^{-1}\mathbf{z}\;\leq\;\frac{1}{4}(\alpha_s+k_s)^2(\boldsymbol{\eta}-k_g\mathbf{q}_{\mathbf{m}})^{\mathrm{T}}\mathbf{V}(\boldsymbol{\eta}-k_g\mathbf{q}_{\mathbf{m}})+\mathbf{z}^{\mathrm{T}}\mathbf{D}^{-1}\mathbf{V}^{-1}\mathbf{D}^{-1}\mathbf{z}\qquad(37)$$

where $\mathbf{V}$ is a positive definite matrix.

Finally, $\dot{V}$ can be written considering equations (28)-(37) in the following way:

$$\begin{aligned}\dot{V}&=\dot{V}_1+\dot{V}_2+\dot{V}_3+\dot{V}_4+\dot{V}_5\\&\leq\dot{\mathbf{q}}_{\mathbf{m}}^{\mathrm{T}}\mathbf{B_1}\dot{\mathbf{q}}_{\mathbf{m}}+(\boldsymbol{\eta}-k_g\mathbf{q}_{\mathbf{m}})^{\mathrm{T}}\mathbf{B_2}(\boldsymbol{\eta}-k_g\mathbf{q}_{\mathbf{m}})+\mathbf{z}^{\mathrm{T}}\mathbf{B_3}\mathbf{z}+\mathbf{z}^{\mathrm{T}}\mathbf{D}^{-1}\mathbf{f_e}+(\boldsymbol{\eta}-k_g\mathbf{q}_{\mathbf{m}})^{\mathrm{T}}\mathbf{D}^{-1}\mathbf{f_e}\\&\quad+\frac{k_g}{k_m}\dot{\mathbf{q}}_{\mathbf{m}}^{\mathrm{T}}\mathbf{f_a}+\gamma k_gh_2\sigma\left|\dot{\mathbf{q}}_{\mathbf{m}}\right|-k_s(\boldsymbol{\eta}-k_g\mathbf{q}_{\mathbf{m}})^{\mathrm{T}}\mathbf{D}^{-1}\mathbf{u_k}-k_s\mathbf{z}^{\mathrm{T}}\mathbf{D}^{-1}\mathbf{u_k}\\&\leq\dot{\mathbf{q}}_{\mathbf{m}}^{\mathrm{T}}\mathbf{B_1}\dot{\mathbf{q}}_{\mathbf{m}}+(\boldsymbol{\eta}-k_g\mathbf{q}_{\mathbf{m}})^{\mathrm{T}}\mathbf{B_2}(\boldsymbol{\eta}-k_g\mathbf{q}_{\mathbf{m}})+\mathbf{z}^{\mathrm{T}}\mathbf{B_3}\mathbf{z}+c_1\left|\dot{\mathbf{q}}_{\mathbf{m}}\right|+c_2\left|\boldsymbol{\eta}-k_g\mathbf{q}_{\mathbf{m}}\right|+c_3\left|\mathbf{z}\right|\end{aligned}\qquad(38)$$

being

$$\begin{aligned}\mathbf{B_1}&=-\frac{(\alpha_m+\alpha_h)\,k_g}{k_m}\mathbf{I}+\frac{1}{4}k_g^2\bar{h}_2\mathbf{W}^{-1}+\bar{h}_1(\mathbf{X}+\mathbf{Y})\\\mathbf{B_2}&=-k_s\mathbf{D}^{-1}+\frac{1}{4}(\alpha_s+k_s)^2\mathbf{V}+\;\frac{1}{4}\bar{h}_1k_g^2k_s^2\mathbf{D}^{-1}\mathbf{X}^{-\mathbf{1}}\mathbf{D}^{-1}\\\mathbf{B_3}&=-\alpha_s\mathbf{D}^{-1}-\mathbf{I}+\mathbf{D}^{-1}\mathbf{V}^{-1}\mathbf{D}^{-1}+\bar{h}_2\mathbf{W}+\;\frac{1}{4}\bar{h}_1k_g^2k_s^2\mathbf{D}^{-1}\mathbf{Y}^{-1}\mathbf{D}^{-1}\\c_1&=\frac{k_g}{k_m}\bar{f}_a+\gamma k_gh_2\sigma,\qquad c_2=c_3=\frac{\bar{f}_e+k_su_m}{\lambda_{min}(\mathbf{D})}\end{aligned}$$

with $\mathbf{I}$ the identity matrix and $\lambda_{min}(\mathbf{D})$ the minimum eigenvalue of matrix $\mathbf{D}$.

The controllers parameters $(k_m, k_s, \alpha_m, \alpha_s)$ can be set to guarantee that $\mathbf{B_1}$, $\mathbf{B_2}$ and $\mathbf{B_3}$ are negative definite and, therefore, $\dot{V}(t)$ is negative outside a compact set $\Omega(\mathbf{x})$. This implies the state $\mathbf{x}$ is bounded for all t ($\mathbf{x} \in \mathcal{L}_\infty$).

Remark 4: If components c_1, c_2, c_3 are null, then the system is stable. For this particular case, Barbalat's lemma can be used in (38), taking into account assumptions 1 and 2, property 3 and the fact that $\mathbf{x} \in \mathcal{L}_\infty$ (and also $\boldsymbol{\eta} \in \mathcal{L}_\infty$), it is possible to deduce that $\ddot{\mathbf{q}}$, $(\dot{\boldsymbol{\eta}} - k_g \dot{\mathbf{q}}_\mathbf{m})$ and $\dot{\mathbf{z}}$ are bounded; then $\ddot{V}$ is bounded too. Finally, $\dot{\mathbf{q}}$, $(\boldsymbol{\eta} - k_g \mathbf{q}_\mathbf{m})$ and $\mathbf{z}$ will tend to zero as $t \to \infty$.

6. Performance Measures

Unlike conventional teleoperation like telesurgery, hard contact between the mobile robot and obstacles is undesired in many task related with supervision and transportation. Consequently, there are no actual physical forces to be transmitted to the master, and the conventional objectives of force tracking are not applicable. For this reason, common evaluation metrics like pure force tracking and classical transparency [12] are not suitable for the kind of teleoperation task analysed in this paper; therefore, some others metrics need to be introduced.

In a teleoperated system, not only task performance is important, but also sensibility to different operators and conditions of operation. Next, we described some evaluation metrics.

6.1. *Task Performance*

1) *Time to complete the task*: In conventional teleoperation research, the position tracking ability of the slave is typically evaluated by estimating the discrepancy between the position of the slave and the master. Others, in similar tasks (to guide a robot or team of robots avoiding obstacles) as the one presented in this paper, propose to measure the discrepancy between the position of the slave and the target position on the reference path that the teleoperator intends to maneuver to [22].

In this work, the concern is over: 1) the discrepancy between the path made by the robot and the shorter path (the reference path is proposed to be the shorter one), and 2) the speed of the robot (high speeds are preferred). So, we do not want unnecessary reductions of the robot's mobility by the remote controller.

$$T_{task} := \text{time that it takes the robot to go from A to B} \tag{39}$$

2) *High collision probability*: On one hand, the main task is required to be as quickly as possible (evaluated by T_{task}) while on the other hand, obstacles over the path represents restrictions to the movement of the robot. Hence, this index is about the risk the robot faces. We describe this evaluation metric as

$$HCP = \frac{1}{n_{ob}} \sum_{i=1}^{n_{ob}} \left(\frac{1}{T_{exp}} \int_0^{T_{exp}} P_i^3(t) dt \right) \tag{40}$$

where n_{ob} is the quantity of obstacles, i represent the obstacle subindex, T_{exp} is the time of the experiment, and P_i is the collisions probability of the robot against the obstacle i. Designers can use any method for computing the collision probability. We use the method explained in section 4.2, which is base on a linear integration of the velocities (velocity in the x and y coordinates of the plane) of the robot and obstacle. The cubic function of the collision probability is chosen, due

to it *enhances high values* of risk (high collision probabilities attempt to the safety of the mission) and *reduces the low values* (not important for evaluating risk).

6.2. *Heterogeneous commands*

It is reasonable to think that a system developed under the human-centered design concept, should include in its evaluation some indexes that highlight undesirable differences in performance. These differences appear when the system is teleoperated by different human operators, or by the same pilot under dissimilarities conditions that affect the command execution, e.g., workload, distractions, inexperience, undesired command executions, poor perception of the environment, etc. In order to achieve a quantitative value that highlights these differences over the task performance, the following equations based on the discrete standard deviation are proposed:

3) *Deviation in time to complete the task*:

$$\sigma_{tt} = \sqrt{\frac{1}{N-1}\sum_{b=1}^{N}(T_{task_b} - \overline{T_{task}}\ )^2} \tag{41}$$

where N is the quantity of tests done, b is the number of the test, T_{task_b} is the T_{task} for the test b while $\overline{T_{task}}$ is the average.

4) Deviation in high collision probabilities:

$$\sigma_{hcp} = \sqrt{\frac{1}{N-1}\sum_{b=1}^{N}(HCP_b - \overline{HCP})^2} \tag{42}$$

where N is the quantity of tests done, b is the number of the test, HCP_b is the HCP for the test b while $\overline{HCP}$ is the average.

Both evaluation metrics should be higher when variance between experiments is high. If the system do really face the issue of heterogeneity of the commands, the variance (or standard deviation) of them should be lower than others systems without a consideration of it.

Generally in teleoperation systems, not only stability is important but also transparency is an aspect to be taken into account, which represents how accurate the operator perceives the environment. A previous work of [34] propose a criterion called absolute transparency to measures how and how fast the human operator and the remote system interact with each other, so different control schemes can be compared in this sense. In our case, collision avoidance method of the remote controller can change the command sent. So, we propose to evaluate this quantitatively, therefore, the following metric is proposed:

5) *Command feeling*:

$$V_{t_j} = \frac{\int_0^{T_{exp}} u_{h_j}(t)\ \eta_j(t)\ dt}{\sqrt{\int_0^{T_{exp}} u_{h_j}^2(t)\ dt}\ \sqrt{\int_0^{T_{exp}} \eta_j^2(t)\ dt}} \tag{43}$$

with $j = 1; 2$, being $\eta = [\eta_1\ \eta_2]$ the measured linear and angular robot velocity and $u_h = [u_{h_1}\ u_{h_2}]$ the linear and angular received commands in the remote site.

7. Experimentation

The experimentation was divided in two parts, called Exp_A and Exp_B. Both consist on a teleoperation of a mobile robot Pioneer 3AT (from Adept MobileRobots) through Ethernet. In Exp_A, a local network *(LAN) with addition of simulated time delay* was utilized; while in Exp_B, the communication was performed *over the Internet (WAN), between the National University of San Juan (Argentina) and the University of Verona (Italy).*

7.1. *Participant*

For Exp_A, 10 participants (age range: 20 - 55 years) from the National University of San Juan took part in these experiments. None presented any physical disability. For the experiment Exp_B, one user from the National University of San Juan located in the University of Verona was asked to drive the mobile robot.

Participants were experts and non-experts. Finally, instructions on manipulating the haptic device and experimental procedure were presented to all the users on a pre-experiment windows information.

7.2. *Equipment*

The equipment mainly consist of a main display and a haptic device at the local site, a common Internet connection, and a Pioneer 3AT mobile robot with a closed-loop speed control at the remote site. The display shows the video transmitted from the remote site.

Sample time at the local site for the master device was $10ms$ due to $\dot{\mathbf{q}}$ computation and damping force feedback ($\alpha_m \dot{\mathbf{q}}$). Data transmission rate and sample time at the remote site were made at $50ms$.

A commercial haptic device (Novint Falcon) was used as the master device. It is a 3DOF translational joystick (only 2DOF were used), with force feedback.

The position of the obstacles is known, as well as its size (ε_{dst} of each obstacle). In future works, it is possible to add a laser sensor to measure the relative distance to obstacles. But, for this work, it is better to have a well structured test thus errors in the position estimation algorithm do not interfere with results.

7.3. *Channel Time Delay*

1) In experiment Exp_A, a simulated channel delay was added to the LAN, therefore, there was repeatability in the teleoperation conditions. Although the time delay is simulated for this case; the operator, visual feedback, master device and robot dynamics are real. Eq. (44) shows the forward and a backward time delays (h_1 and h_2) considered.

$$\begin{cases} h_1 = 0.30 \\ h_2 = 0.1 * \sin(0.5 * t) + 0.3 \end{cases} \tag{44}$$

2) In experiment Exp_B, h_1 and h_2 were measured and averaged in order to have a mean value of the total time delay involved:

$$450ms < h_{1+2} < 860ms \tag{45}$$

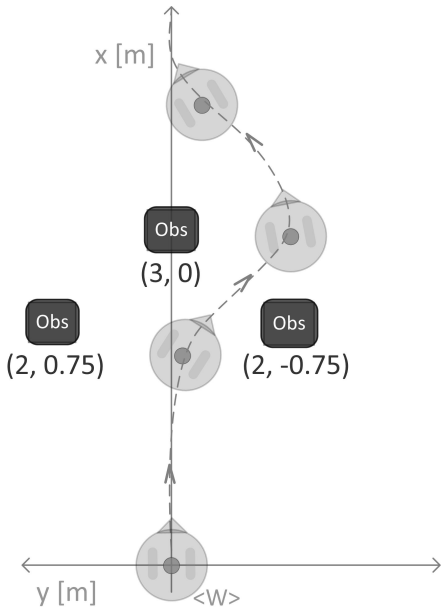

Figure 5. Environment and Path to follow

7.4. *Control Parameters*

In the stability analysis, parameters k_g, k_s, α_s, k_m, α_m, u_m and k_f where considered as scalar due to simplicity, but the analysis and results are also valid for positive definite diagonal matrices.

The closed-loop speed controller included in the mobile robot's control board was previously well adjusted, therefore, speed references send to the robot are expected to be well followed.

The parameters k_m, k_g, and k_s are set empirically since they are independent on the time delay. From this and the maximum values of h_1 and h_2, the stability condition should be solved to find the tuning parameters of α_m and α_s. For the master device controller, we set $k_m = diag\{20\frac{Ns}{m};\ 3\frac{Ns}{m}\}$ and $\alpha_m = diag\{10\frac{Ns}{s};\ 10\frac{Ns}{m}\}$.

In order to transform the position of the master to a speed reference, k_g is established as $k_g = diag\{10.0\frac{1}{s};\ 5.0\frac{1}{s}\}$ The range of the master position in both axis is from $-0.05[m]$ to $0.05[m]$, so, the linear and angular maximum speed references are $0.5[\frac{m}{s}]$ and $0.25[\frac{rad}{s}]$. Finally, u_m was set to $u_m = diag\{0.35;\ 0.20\}$.

7.5. *Procedure*

In the experiments, participants were required to maneuver a mobile robot using the haptic control device while seeing the robot's onboard camera video on the screen. The path to be followed by the robot was difficult due to obstacles positions. In order to compare our proposal with null-gain and constant-gain velocity impedance controllers, three impedance laws were set:

- (A) $\mathbf{u_k} = 0$,
- (B) $\mathbf{u_k} = sgn(\mathbf{q_m}(t-h1))u_m(1-e^{-(\varepsilon+0.8)k_f\mathbf{f_e}})$, (constant-gain)
- (C) $\mathbf{u_k} = sgn(\mathbf{q_m}(t-h1))u_m(1-e^{-(\varepsilon+C_{Met})k_f\mathbf{f_e}})$, (metric-dependent variable-gain).

Before starting the experimentation, a tutorial and training session were provided to each participant in order to get them familiarized with the Novint device and with the procedure.

The environment with obstacles and path to be followed by the robot are shown in figure 5. The robot is approximately $0.4m$ by $0.45m$, and the obstacles $0.35m$ by $0.35m$ (all of them are fixed). Central point coordinates of each obstacle are shown in the figure. As the free space between obstacles is narrow with respect to the robot's dimension, it is difficult to pass through them taking into account time delays and velocity of the robot. The task presents complex driving maneuvers

Table 1. Table of variables measured in the experiments

Case	T_{task} $[s]$	HCP	σ_{tt}	σ_{hcp}	V_{t_1}	V_{t_2}
A	76.57	0.0080	13.84	0.004	0.887	0.952
B	126.27	0.0001	7.53	0.00022	0.817	0.851
C	78.92	0.0002	6.88	0.00009	0.889	0.954

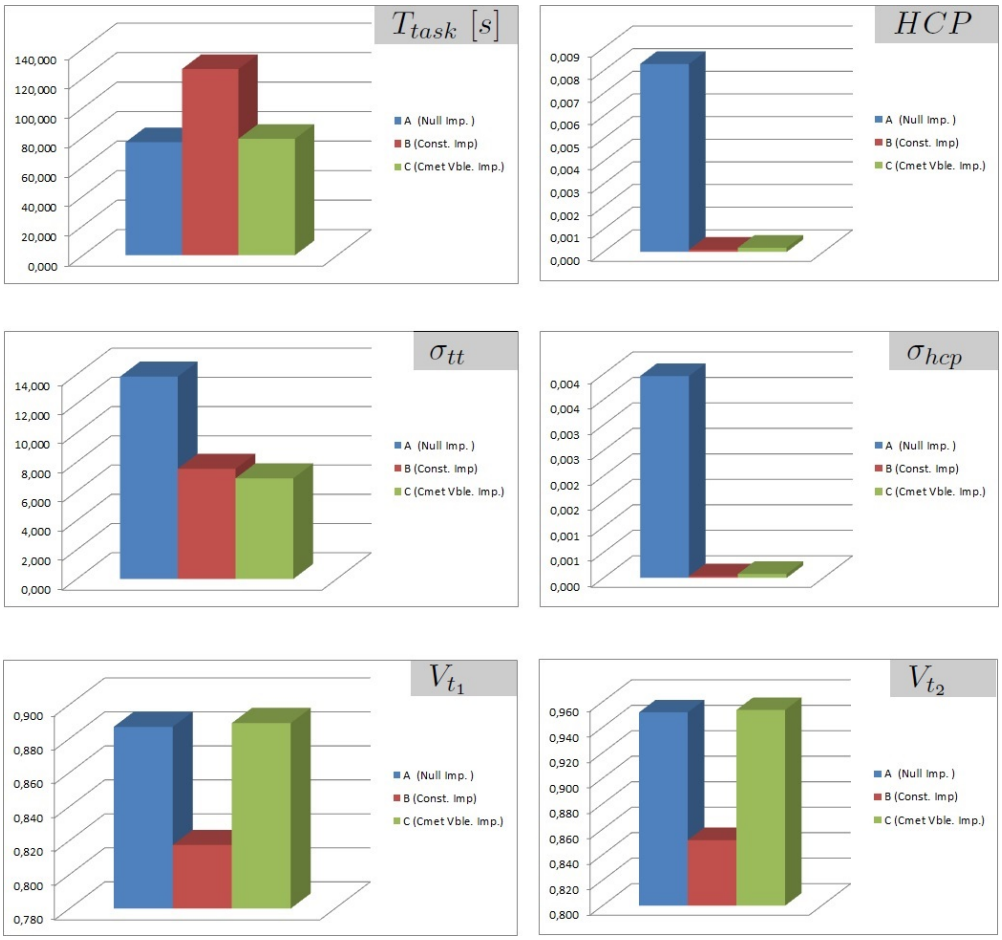

Figure 6. Evaluation metrics values of Exp_A

which results in high collision probabilities when bad commands are applied.

7.6. *Results*

7.6.1. Experiment Exp_A

Table 1 presents a summary of the evaluation metrics proposed in section 6. The data correspond to the average scores of 10 participant that performed the task using schemes A, B and C (Exp_A). Participants were experts and non-experts.

Figure 6 presents a graphical representation of the table 1 in order to help the readers' understanding.

The third case (**C**) performs an intelligent trade-off between the first (**A**) and second (**B**) cases based on command performance according to collision probability. **A** has some advantages as well as **B**, so, we want to analyze how well **C** takes advantages of both. It is know in the teleoperation field that schemes in direct mode like **A** are quite good for expert users and dangerous for inexperienced ones, while in high conservative schemes like **B** the opposite applies. A more deep analysis on the schemes' performances shows that **C** has a better trade-off between the evaluation metrics.

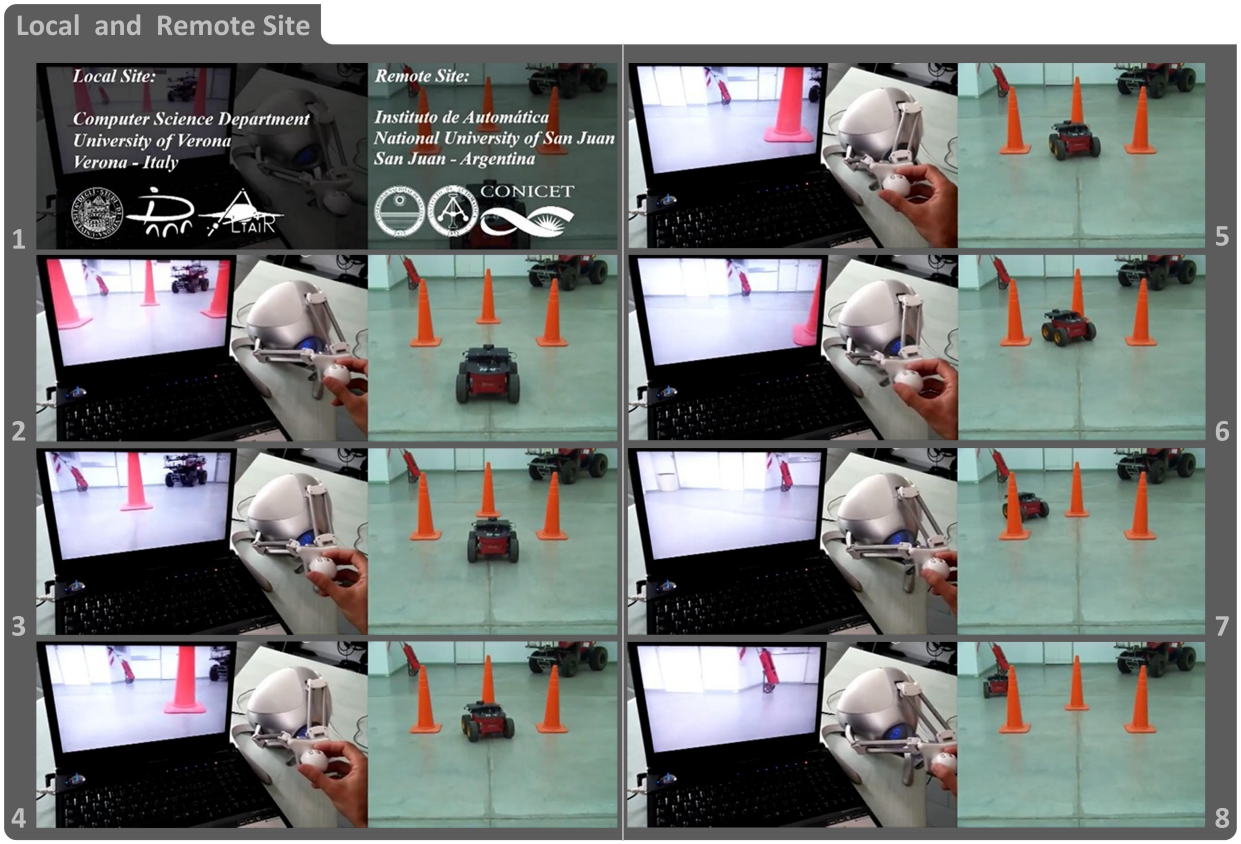

Figure 7. Screenshots of the local (University of Verona) and remote site (National University of San Juan). **C Scheme**

Comparing **C** to **A** and **B**, it can be seen that:

1) T_{task} in **C** is considerably lower than in **B**, and similar to T_{task} in **A** (good drivers can apply good times since the remote controller never stops the commands).

2) HCP in **C** is a bit higher than in **B** (which is reasonable since **B** scheme is the most conservative one), but much lower than in **A**. **A** and **B** schemes have the advantage to be safe.

3) σ_{tt} and σ_{hcp} in **C** are much lower than in **A** and closer to the ones in **B**, which indicates that the scheme is less sensitive to the variability of the commands execution (variability in the sense of obstacles avoidance). $\sigma_{tt,hcp}$ are advantages of **B**.

4) V_{t_1} and V_{t_2} are bigger in **C** (very close to the ones measured in **A**) than in **B**, indicating that the user can feel a better tracking of his commands. This is possible since the impedance is proportional to the *wrongness* of the human directives about risk, and not always applied like in **B**. High $V_{t_{1,2}}$ are advantages of **A**.

7.6.2. Experiment Exp_B

For Exp_B, we have performed a teleoperation test for each scheme under analysis with the local site on Verona-Italy and the remote site on San Juan-Argentina. Videos of the experiments can be seen in `https://plus.google.com/115750055928123003273/posts/NMJAVLEyXYd`, where the first video correspond to **A** scheme driven by an expert user and the second and third videos correspond to **B** and **C** (novel proposal of this work) schemes respectively.

Figure 7 presents multiple screenshots of the local and remote site of the teleoperation system (**C** scheme).

Figure 8 shows the trajectory followed by the robot and the obstacles, were the darkness of each point represent the experiment's time for each sample (the more dark, the more late).

On the local site, the torque applied to the master for both axis (linear and angular) are shown

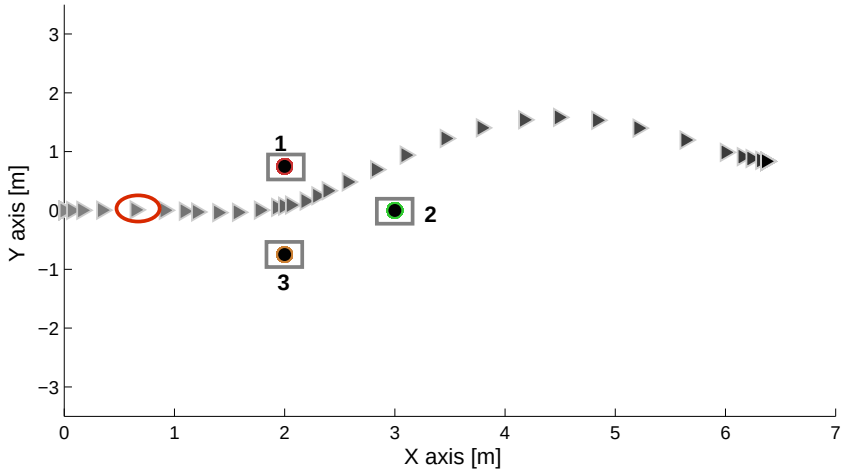

Figure 8. Robot's trajectory (triangles) and obtacles' position (circles).

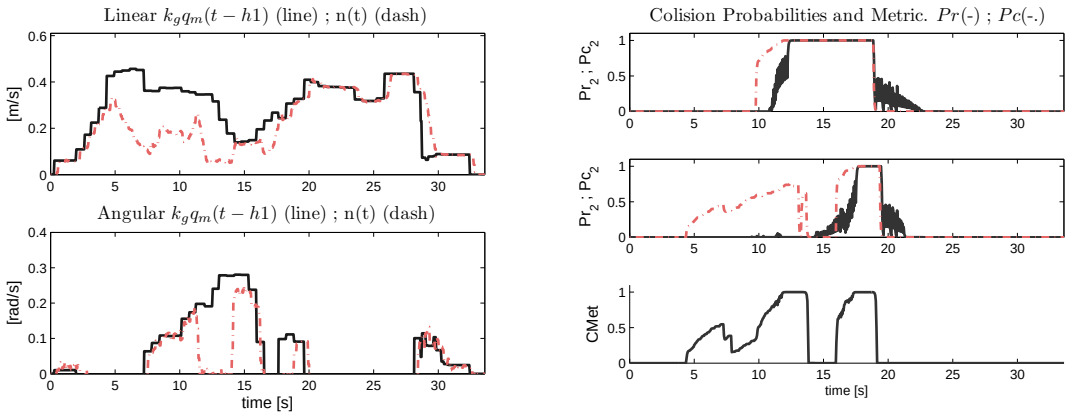

(a) Human commands after h_1 ($k_g q_m(t-h_1)$) and robot's output

(b) Real and command collision probabilities of the robot against each obstacle, and metric computation

Figure 9. Data at the remote site (San Juan - Argentina)

in figure 10(a). In addition, figure 10(b) shows that $\dot{\mathbf{q}}$ is bounded for all time.

Referring to the remote site, the impedance reduces the intensity of the commands applied in some moments(like at time $t \approx 10s$), depending on the value of the proposed metric (figure 9(b)). As a result of this, the robot's dynamics and the channel delays, velocities (linear and angular) reached by the robot are different with respect to the human commands references (figure 9(a)).

Furthermore, figure 9(b) exposes the real and command collision probabilities of the robot against each obstacle (collisions against obstacle 3 is not shown because it is zero for all time), as well as the computation of the proposed command metric. It can be observed at $t \approx 11s$ that the metric is high because the command tends to worsen the collision probability situation against obstacle 1. At $t \approx 17.5s$ the situation is undetermined due to Pr is higher and the command can not improve the risk situation. At $t \approx 20s$, the command tends to improve the situation, thus the metrics tend to zero and the impedance do not reduce the energy of the command sent by the human operator.

8. Discussion

It is well known in delayed teleoperation of mobile robots that in order to prevent collisions with obstacles, the remote controller should assist the slave vehicle. In table 1, Case **A** presents the

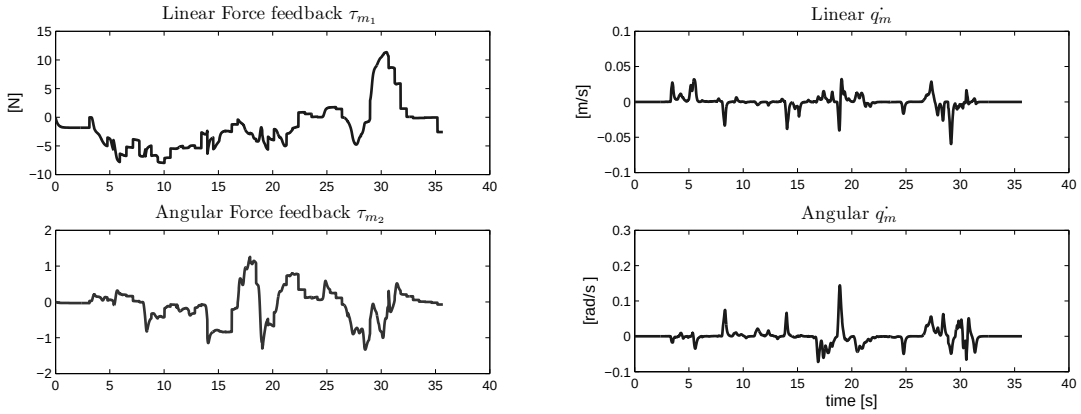

(a) Applied torque to the Master (b) Speed of the Master

Figure 10. Data on Local Site (Verona - Italy)

higher values of collision probabilities and standard deviations. Good drivers achieve good task performance, while bad or distracted drivers have poor task performances. In this case, task execution is highly dependent on the operator's command. On the other hand, a fixed-gain impedance controller (case **B**), slows down the robot's velocity when approaching an obstacle despite how good or bad operator's commands are. This makes the navigation always safer but also increases the time to complete the task and reduces the transparency of the command operator. This scheme wastes good commands.

On the contrary, in the proposal presented in this work (case **C**), conditions of safety driving do not depend strongly on the operator's received commands performance. Thus, collisions are mitigated at a cost of losing transparency but only when bad commands are estimated by the proposed metric (C_{Met}). Furthermore, good commands are not wasted since they are not compensated, which lead to a low T_{task}, maintaining a safe navigation. In addition, standard deviations are the lowest, indicating a more homogeneous accomplishment of the task despite user's distractions and driving-experience differences.

9. Conclusions

In this paper we have presented a mobile robot teleoperation system under asymmetric time-varying delays, in which the control law considers a metric of a human factor. A haptic cue and a compensation of the sent commands, help the human operator when he applies wrong directives that could cause collisions. For this purpose, we have proposed and implemented an on-line risk-based quantitative metric considering the human command performance in the form of a variable-gain impedance control law. Although in this work we have proposed and tested the inclusion of this metric in an impedance-based remote controller, the metric can be used in different control schemes to improve its performance. We also have proposed some performance metrics to compare this novel control scheme against others in a more broadly sense. In addition, a Lyapunov-based stability analysis of the teleoperation system has been developed.

Results of the HITL simulations and experiments with human operators allow us to ensure that, on the one hand, the proposed scheme has a better trade-off between safety, transparency, and time to complete the task and, on the other hand, the systems is less sensitive to bad commands showing robustness in front of undesirable aspects that can affect the human operator during a mobile robot teleoperation task.

In addition, an intercontinental teleoperation of a Pioneer 3AT was performed, with the local site in the University of Verona and the Remote Site on the University of San Juan.

ACKNOWLEDGEMENTS

This work was supported by the Consejo Nacional de Investigaciones Científicas y Técnicas (CONICET), the National University of San Juan and the Automatics Institute of the National University of San Juan. We also thanks the University of Verona and Professor Paolo Fiorini for his collaboration on this work.

References

[1] T. B. Sheridan, *Telerobotics, Automation, and Human Supervisory Control*. MIT Press Cambridge, MA, USA, 1992.
[2] T. B. Sheridan, *Telerobotics, Automation and Human Supervisory Control*. MIT Press, 1992.
[3] C. Sayers, *Remote control robotics*. Springer-Verlag, 1999.
[4] L. Slutski, *Remote manipulation systems: quality evaluation and improvement*. Kluwer Academic Publishers, 1998.
[5] P. Fiorini and R. Oboe, "Internet-based telerobotics: Problems and approaches," 1997.
[6] I. Elhajj, N. Xi, W. K. Fung, Y.-H. Liu, Y. Hasegawa, and T. Fukuda, "Supermedia enhanced internet based telerobotics," *Proceedings of the IEEE*, vol. 91, pp. 396–421, 2003.
[7] T. M. Lam, H. W. Boschloo, M. Mulder, and M. M. van Paassen, "Artificial force field for haptic feedback in uav teleoperation," *IEEE Transactions on Systems, Man, and Cyberneteics-Part A: Systems ans Humans*, vol. 39, pp. 1316–1330, 2009.
[8] D. Sanders, "Comparing ability to complete simple tele-operated rescue or maintenance mobile-robot tasks with and without a sensor system," *Sensor Review*, vol. 30, pp. 40 – 50, 2010.
[9] P. F. Hokayem and M. W. Spong, "Bilateral teleoperation: An historical survey," *Automatica*, vol. 42, no. 12, pp. 2035–2057, 2006.
[10] J. P. Richard, "Time-delay systems: An overview of some recent advances and open problems," *Automatica*, vol. 39, no. 10, pp. 1667–1694, 2003.
[11] T. B. Sheridan, "Space teleoperation through time delay: Review and prognosis," *IEEE Trans. Robot. Autom.*, vol. 9, no. 5, pp. 592–606, 1993.
[12] D. A. Lawrence, "Stability and transparency in bilateral teleoperation," *IEEE Trans. Robot. Autom.*, vol. 9, no. 5, pp. 624–637, 1993.
[13] C. D. Wickens and J. G. Hollands, *Engineering Psychology and Human Performance - 3 edition*, vol. 1. New Jersey 07458: Prentence Hall, 2000.
[14] J. Daly and D. Wang, "Time-delayed output feedback bilateral teleoperation with force estimation for n -dof nonlinear manipulators," *Control Systems Technology, IEEE Transactions on*, vol. 22, pp. 299 – 306, 2014.
[15] B. Willaert, D. Reynaerts, H. Van Brussel, and E. Poorten, "Bilateral teleoperation: Quantifying the requirements for and restrictions of ideal transparency," *Control Systems Technology, IEEE Transactions on*, vol. 22, pp. 387 – 395, 2014.
[16] W. Yamanouchi and S. Katsura, "Tele-operation of a mobile haptic system using dynamical modal transformation," *IEEJ Transactions on Industry Applications*, vol. 132-D, pp. 315–321, 2012.
[17] S. Sakaino, T. Sato, and K. Ohnishi, "A novel motion equation for general task description and analysis of mobile-hapto," *Industrial Electronics, IEEE Transactions on*, vol. 60, no. 7, pp. 2673–2680, 2013.
[18] J. Chen, E. Haas, and M. Barnes, "Human performance issues and user interface design for teleoperated robots," *Systems, Man, and Cybernetics, Part C: Applications and Reviews, IEEE Transactions on*, vol. 37, no. 6, pp. 1231–1245, 2007.
[19] E. S. Jang, S. Jung, and T. Hsia, "Collision avoidance of a mobile robot for moving obstacles based on impedance force control algorithm," in *Intelligent Robots and Systems, 2005. (IROS 2005). 2005 IEEE/RSJ International Conference on*, pp. 382–387, Aug 2005.
[20] E. Slawiñski, V. Mut, L. Salinas, and S. García, "Teleoperation of a mobile robot with time-varying delay and force feedback," *Robotica*, vol. 30, pp. 67–77, January 2011.
[21] F. Janabi-Sharifi, , and I. Hassanzadeh, "Experimental analysis of mobile-robot teleoperation via shared impedance control," *IEEE TRANSACTIONS ON SYSTEMS, MAN, AND CYBERNETICSPART B: CYBERNETICS,*, vol. 41, pp. 591–606, April 2011.

[22] H. I. Son, A. Franchi, L. L. Chuang, J. Kim, H. H. Blthoff, and P. R. Giordano, "Human-centered design and evaluation of haptic cueing for teleoperation of multiple mobile robots," *IEEE Transactions on Cybernetics*, vol. 43, no. 2, pp. 597–609, 2013.

[23] S. K. Cho, H. Z. Jin, J. M. Lee, , and B. Yao, "Teleoperation of a mobile robot using a force-reflection joystick with sensing mechanism of rotating magnetic field," *IEEE/ASME TRANSACTIONS ON MECHATRONICS*, vol. 15, pp. 17–26, February 2010.

[24] I. Farkhatdinov, J.-H. Ryu, and J. An, "A preliminary experimental study on haptic teleoperation of mobile robot with variable force feedback gain," in *Haptics Symposium, 2010 IEEE*, pp. 251–256, March 2010.

[25] F. Penizzotto, E. Slawiñski, and V. Mut, "Teleoperation of mobile robots considering human's commands," in *ROBOT2013: First Iberian Robotics Conference. Advances in Intelligent Systems and Computing* (M. Armada, A. Sanfeliu, and M. Ferre, eds.), vol. 253, pp. 601–614, Springer, 2014.

[26] E. Nuño, R. Ortega, N. Barabanov, and L. Basañez, "A globally stable PD controller for bilateral teleoperators," *IEEE Trans. Robot.*, vol. 24, no. 3, pp. 753–758, 2008.

[27] C.-C. Hua and X. Liu, "Delay-dependent stability criteria of teleoperation systems with asymmetric time-varying delays," *IEEE Trans. Robot.*, vol. 26, no. 5, pp. 925 –932, 2010.

[28] E. Slawiñski and V. Mut, "Pd-like controllers for delayed bilateral teleoperation of manipulators robots," *International Journal of Robust and Nonlinear Control*, 2014.

[29] E. Slawiñski, V. Mut, and J. Postigo, "Teleoperation of mobile robots with time-varying delay," *IEEE Transaction on robotics*, vol. 23, 2007.

[30] K. Hashtrudi-Zaad and S. E. Salcudean, "Analysis of control architectures for teleoperation systems with impedance/admittance master and slave manipulators," *The International Journal of Robotics Research*, vol. 20, no. 6, pp. 419–445, 2001.

[31] D. Chavez, E. Slawinski, and V. Mut, "Collaborater for car-like vehicle driven by a user with visual inattention," *Asian Journal of Control*, vol. 15, p. 177192, 2013.

[32] S. I. Niculescu, *Delay Effects on Stability: A Robust Control Approach*. Springer Verlag, 2001.

[33] E. Slawiñski, V. A. Mut, and J. F. Postigo, "Stability of systems with time-varying delay," *Latin American applied research*, vol. 36, pp. 41–48, 2006.

[34] E. Slawiñski, V. A. Mut, P. Fiorini, and L. R. Salinas, "Quantitative absolute transparency for bilateral teleoperation of mobile robots," *IEEE Transactions on Systems, Man and Cybernetics, Part A: Systems and Humans*, vol. PP, no. 99, pp. 1 –13, 2012.